

**CHAPTER I:  $\gamma$ 1-Adaptin Interacts  
Directly with Rabaptin-5 through Its Ear  
Domain**

## ABSTRACT

In a yeast two-hybrid screening using  $\gamma$ 1-adaptin, a subunit of the AP-1 adaptor complex of clathrin-coated vesicles derived from the TGN, as a bait, I found that it could interact with Rabaptin-5, which is an effector of Rab5 and Rab4 and regulates membrane docking with endosomes. A further two-hybrid analysis revealed that the interaction occurred between the ear domain of  $\gamma$ 1-adaptin and the COOH-terminal coiled-coil region of Rabaptin-5. Pull down assay with a fusion protein between glutathione *S*-transferase and the ear domain of  $\gamma$ 1-adaptin and coimmunoprecipitation analysis revealed that the interaction occurred *in vitro* and *in vivo*. Immunocytochemical analysis showed that  $\gamma$ 1-adaptin and Rabaptin-5 were significantly colocalized on perinuclear structures, probably on recycling endosomes, and were redistributed into the cytoplasm upon treatment with brefeldin A. These results suggest that the  $\gamma$ 1-adaptin-Rabaptin-5 interaction may play a crucial role in docking of clathrin-coated vesicles derived from the TGN with endosomes or of those from endosomes with the TGN.

## INTRODUCTION

The TGN is the major sorting station of the biosynthetic pathway, in which newly synthesized soluble and transmembrane proteins, as well as lipids, are sorted for subsequent transport to different destinations. Clathrin/AP-1-coated vesicles mediate vesicular transport from the TGN to endosomes.

In clathrin/AP-2-coated vesicle, the ear domain of  $\alpha$ -adaptin, a large subunit of the AP-2 complex, is capable of interacting with a wide variety of cytosolic accessory molecules that regulate the endocytic processes. To explore the regulatory mechanism underlying the transport from the TGN to endosomes, I searched for binding proteins of  $\gamma$ 1-adaptin, which is a counterpart of  $\alpha$ -adaptin in the AP-1 complex.

In a yeast two-hybrid screening using  $\gamma$ 1-adaptin as bait, I found that it could interact with Rabaptin-5, which is an effector of Rab5 and Rab4 and regulates membrane fusion with endosomes.

The molecular machineries regulating docking and fusion of membranes have been elucidated in the past few years. NSF (*N*-ethylmaleimide-sensitive factor), SNAREs (soluble NSF attachment protein receptors) and Rab family of small GTPases have been assigned special roles in these processes (for review, see Refs. 46, 47). The Rab family amounts to more than 60 members in mammalian cells which exert functions in different trafficking steps in the exocytic and endocytic pathways (reviewed in Refs. 48, 49). Among them, most extensively studied is Rab5. Rab5 has been shown to regulate docking and fusion of early endosomes by interacting with various effector molecules, such as Rabaptin-5, early endosomal autoantigen 1 (EEA1) and phosphoinositide 3-kinases (50-53). Recent evidence indicates that the oligomeric complex containing EEA1, Rabaptin-5, Rabex-5 and NSF drives membrane fusion via interactions between EEA1 and SNAREs, syntaxin 13 and syntaxin 6 (54, 55). Although Rabaptin-5 was originally identified by its interaction with Rab5 (50), Rabaptin-5 and its variant, Rabaptin-4, were then

shown to interact with Rab4 as well (56, 57). Rab5 and Rab4 associate with distinct but partially overlapping endosomal structures and may regulate distinct fusion processes (58-60). Rabaptin-5 is an effector of small GTPase Rab5 and Rab4 and regulates membrane docking with endosomes

Therefore, it is possible that the interaction between  $\gamma$ 1-adaptin and Rabaptin-5 modulates the transport of the clathrin/AP-1-coated vesicles from the TGN to endosomes (Fig. I-1). Here, I provide the first evidence for a direct interaction between  $\gamma$ -adaptins and Rabaptin-5, and address the physiological relevance of the interaction.

## MATERIALS AND METHODS

*Plasmid Construction* — For use in yeast two-hybrid analyses, a bait vector for human  $\gamma$ 1-adaptin (pGBT- $\gamma$ 1) was constructed as described previously (15). Bait vectors for deletion mutants of human  $\gamma$ 1-adaptin ( $\gamma$ 1-head, amino acid residues 1-594; and  $\gamma$ 1-ear, amino acid residues 706-822),  $\gamma$ 2-adaptin ( $\gamma$ 2-head, amino acid residues 1-592; and  $\gamma$ 2-ear, amino acid residues 669-785) and mouse  $\alpha$ A-adaptin ( $\alpha$ A-ear, amino acid residues 739-977) were constructed by separate subcloning of corresponding cDNA fragments obtained by polymerase chain reaction (PCR)-based method into pGBT9-BEN (15). Prey vectors for full-length mouse Rabaptin-5 and its deletion mutants (amino acid residues 276-546, 546-862, 546-728 and 662-862) were constructed by separate subcloning of corresponding cDNA fragments obtained by PCR-based method into pGAD10 (CLONTECH Laboratories, Inc., Palo Alto, CA). To prepare glutathione *S*-transferase (GST)-fusion proteins for use in pull down assays, cDNA fragments for  $\gamma$ 1-ear,  $\gamma$ 2-ear and  $\alpha$ A-ear were separately subcloned into pGEX-4T-2 (Amersham Biosciences, Inc, Uppsala, Sweden). Because the fusion protein between GST and the  $\alpha$ A-ear (amino acid residues 739-977), which was used in the two-hybrid analysis, was insoluble in *Escherichia coli* cells, another fusion construct between GST and an  $\alpha$ A-adaptin region covering a portion of the hinge region and the entire ear domain (amino acid residues 653-977) was used. For expression in mammalian cells as an influenza virus hemagglutinin (HA)-tagged protein, full-length mouse Rabaptin-5, human Rab4(Q67L) and human Rab5(Q79L) cDNAs were separately subcloned into pcDNA3-HAN (61) (the resulting plasmids were referred to as pcDNA3-HA-Rbt5, pcDNA3-HA-Rab4(Q67L) and pcDNA3-HA-Rab5(Q79L), respectively).

*Yeast Two-hybrid Analysis* — pGBT- $\gamma$ 1 was transformed using lithium acetate-based method into yeast Y190 cells, which were plated on synthetic medium lacking tryptophan for selection. The transformant was then transformed with a mouse brain MATCHMAKER cDNA library (CLONTECH

Laboratories), which is constructed for use as prey vectors for pGBT9, grown for 8 h in synthetic medium lacking tryptophan, leucine and histidine, and plated on synthetic medium lacking tryptophan, leucine and histidine and containing 25 mM 3-aminotriazole (Wako Pure Chemical Industries, Ltd, Osaka, Japan). After 10 days of incubation, colonies were examined for  $\beta$ -galactosidase activity by use of a replica filter assay. Library plasmids from positive clones were rescued into *E. coli* HB101 cells by plating on leucine-free minimum medium and subsequently analyzed by retransformation tests and DNA sequencing. By screening of approximately  $1 \times 10^6$  transformants, 24 positive clones are obtained. Among them, although 17 clones encoded fragments of  $\sigma 1$ , which is another AP-1 subunits, one of the positive clones was found to code for mouse Rabaptin-5 (amino acid residues 276-862). The rest 6 clones were unknown protein.  $\beta$ -Galactosidase activity was also measured by a liquid culture assay using *o*-nitrophenylgalactopyranoside as a substrate (62). Two-hybrid analysis was also performed with the head or ear domain of  $\gamma 1$ - or  $\gamma 2$ -adaptin or the ear domain of  $\alpha A$ -adaptin as bait and one of the deletion mutants of Rabaptin-5 as a prey.

*Pull Down Assay* — GST-fusion proteins of  $\gamma 1$ -ear,  $\gamma 2$ -ear and  $\alpha A$ -ear were expressed in *E. coli* BL21(DE3) cells and purified using glutathione-Sepharose 4B (Amersham Biosciences). HeLa cells grown at approximately 80% confluence in nine 100-mm dishes were washed twice with ice-cold phosphate-buffered saline (PBS) and homogenized in 1 ml of homogenization buffer (20 mM HEPES, pH 7.2, 100 mM KCl, 2 mM  $MgCl_2$ , 1 mM dithiothreitol, 2 mM EDTA) containing a protease inhibitor mixture (Complete; Roche Diagnostics, Corp., Indianapolis, IN) by 5 sets of 30 strokes with a Dounce homogenizer (Wheaton Science Products, Millville, NJ). The homogenate was centrifuged at 2,500 rpm for 10 min at 4 °C in a microcentrifuge to remove nuclei and unbroken cells. The postnuclear supernatant was centrifuged at 65,000 rpm for 80 min at 4 °C in a Beckman TLA 100.2 rotor. The supernatant was used as a

cytosol fraction. The pellet was then rinsed once with homogenization buffer, solubilized in homogenization buffer containing 1% Triton X-100, and centrifuged at 12,000 rpm for 20 min at 4 °C in a microcentrifuge. The supernatant was used as a membrane fraction. The protein concentration of the cytosol and membrane extracts was adjusted to 0.9 mg/ml with homogenization buffer. The extracts were incubated at 25 °C for 30 min in the presence of 100  $\mu$ M GDP or GTP $\gamma$ S and after the incubation MgCl<sub>2</sub> was added to a final concentration of 7 mM. To reduce non-specific binding, the cytosol and membrane extracts (170  $\mu$ l) were then preincubated overnight at 4 °C with 20  $\mu$ g of GST prebound to glutathione-Sepharose beads and centrifuged at 2,500 rpm for 1 min in a microcentrifuge. The supernatants were then incubated for 3 h at 4 °C with 10  $\mu$ g of the fusion protein (GST- $\gamma$ 1-ear, GST- $\gamma$ 2-ear or GST- $\alpha$ A-ear) prebound to glutathione-Sepharose beads and centrifuged at 2,500 rpm for 1 min. The pelleted beads were washed four times with 300  $\mu$ l of homogenization buffer containing 0.5% Triton X-100, boiled in SDS-PAGE sample buffer, and centrifuged at 2,500 rpm for 1 min. Equivalent volumes of the supernatants were electrophoresed on a 7.5% SDS-polyacrylamide gel and electroblotted onto an Immobilon-P membrane (Millipore Corp. Billerica, MA). The blot was incubated sequentially with monoclonal mouse anti-Rabaptin-5 antibody (Clone 20; BD Biosciences, San Diego, CA) and with horseradish peroxidase-conjugated anti-mouse IgG (Jackson ImmunoResearch Laboratories, Inc, West Grove, PA), and detected using a Renaissance Chemiluminescence reagent *Plus* (Perkin-Elmer Life Science Products, Inc, Wellesley, MA) according to the manufacturer's instruction.

*Coimmunoprecipitation Analysis* — HeLa cells stably expressing HA-tagged Rabaptin-5 was established by transfection of cells with pcDNA3-HA-Rbt5 using the FuGene6 transfection reagent (Roche Diagnostics) and subsequent selection in the presence of 800  $\mu$ g/ml Geneticin (Life Technologies, Inc., Rockville, MD). One (HeLa/HA-Rbt5) of the clones with a moderate Rabaptin-

5 expression level was used for the following experiment. Non-transfected HeLa cells or HeLa/HA-Rbt5 cells grown at approximately 80% confluence in three 100-mm dishes were washed twice with ice-cold PBS and scraped into 0.7 ml of immunoprecipitation buffer (100 mM HEPES, pH 7.2, 1 mM MgCl<sub>2</sub>, 50 mM NaF) containing a protease inhibitor mixture (Complete EDTA-free; Roche Diagnostics). The cells were then homogenized by passage twenty times through a 22-gauge needle and centrifuged at 2,500 rpm for 10 min at 4 °C to remove nuclei and unbroken cells. The protein concentration of the postnuclear supernatant was adjusted to 2.0 mg/ml with immunoprecipitation buffer. The postnuclear supernatant (430 µl) was then incubated with 20 µl of anti-HA-conjugated agarose (HA-Probe; Santa Cruz Biotechnology, Inc, Santa Cruz, CA) or 0.5 µg of monoclonal mouse anti-Rabaptin-5 antibody (Clone 20) at 4 °C for 18 h. The postnuclear supernatant incubated with anti-Rabaptin-5 was then incubated with Protein G-Sepharose 4FF (Amersham Biosciences) at 4 °C for 3 h. The incubation mixture was centrifuged at 2,500 rpm for 10 min at 4 °C in a microcentrifuge. The pellet was washed four times with ice-cold wash buffer (100 mM Tris, pH 8.0, 150 mM NaCl, 0.1% SDS, 0.5% sodium deoxycholate, 0.5% NP-40), boiled in SDS-PAGE sample buffer, electrophoresed on a 7.5% SDS-polyacrylamide gel, and electroblotted onto an Immobilon-P membrane. The blot was incubated sequentially with monoclonal mouse anti-γ1-adaptin antibody (100/3; Sigma, Inc, St. Louis, MO) and with horseradish peroxidase-conjugated anti-mouse IgG, and detected using a Renaissance Chemiluminescence reagent *Plus* according to the manufacturer's instruction.

*Indirect Immunofluorescence Microscopy* — HeLa cells or normal rat kidney (NRK) cells grown in wells of 8-well Lab-Tek II chamber slide (Nunc A/S, Roskilde, Denmark) were fixed and permeabilized as described by Neuhaus *et al.* (63). Briefly, to cells washed twice with ice-cold PBS, cold methanol at -80 °C was added, and the temperature was raised to -20 °C in 30



min. When indicated, the cells were incubated with 5  $\mu\text{g}/\text{ml}$  brefeldin A (BFA) for 1 min prior to fixation. The cells fixed and permeabilized were washed twice with ice-cold PBS, and incubated with PBS at room temperature for 20 min, then with PBS containing 0.1% gelatin at room temperature for 1 h. The cells were then incubated sequentially with a combination of polyclonal goat anti-Rabaptin-5 antibody (Santa Cruz Biotechnology) and monoclonal mouse  $\gamma 1$ -adaptin antibody [100/3 for HeLa cells or clone 88 (BD Biosciences) for NRK cells], and with a combination of Cy3-conjugated anti-goat and FITC-conjugated anti-mouse IgGs (Jackson ImmunoResearch Laboratories). To compare the distribution of  $\gamma 1$ -adaptin with that of internalized transferrin, HeLa cells were rinsed briefly with a serum-free medium and incubated with Alexa594-conjugated transferrin (a kind gift from Dr. Satoshi Waguri, Osaka University, Japan) at 4  $^{\circ}\text{C}$  for 30 min at a concentration of 5  $\mu\text{g}/\text{ml}$ . Internalization was initiated by replacing the medium with a fresh one prewarmed at 37  $^{\circ}\text{C}$ . At the end of internalization, the cells were rinsed briefly in ice-cold PBS, fixed with 4% paraformaldehyde in PBS at room temperature for 15 min, and permeabilized with 50  $\mu\text{g}/\text{ml}$  digitonin in PBS for 5 min at 4  $^{\circ}\text{C}$ . The cells were then incubated sequentially with monoclonal mouse anti- $\gamma 1$ -adaptin antibody (100/3) and with Alexa488-conjugated anti-mouse IgG (Molecular Probes, Inc, Eugene, OR). To compare the localization of  $\gamma 1$ -adaptin with that of either Rab4(Q67L) or Rab5(Q79L), HeLa cells were transfected with pcDNA3-HA-Rab4(Q67L) or pcDNA3-HA-Rab5(Q79L) using the FuGene6 reagent, incubated for 18 h for the Rab4(Q67L)-transfected cells or for 40 h for the Rab5(Q79L)-transfected cells, fixed and permeabilized with cold methanol. The cells were then incubated sequentially with a combination of monoclonal rat anti-HA antibody (3F10, Roche Diagnostics) and monoclonal mouse anti- $\gamma 1$ -adaptin antibody (100/3), and with a combination of Alexa488-conjugated anti-rat IgG (Molecular Probes) and Cy3-conjugated anti-mouse IgG (Jackson ImmunoResearch Laboratories). The

stained cells were observed with a confocal laser-scanning microscope (TCS-NT; Leica Mikrosysteme, Heidelberg, Germany).

## RESULTS

### *Yeast Two-hybrid Analysis of Interaction between $\gamma$ -Adaptin and Rabaptin-5*

— In order to identify proteins that interact with  $\gamma$  ( $\gamma$ 1)-adaptin, reporter yeast cells were first transformed with a plasmid coding for a fusion protein between the GAL4 DNA-binding domain and full-length  $\gamma$ 1-adaptin (pGBT- $\gamma$ 1; 15). The cells were subsequently transformed with a plasmid mouse brain cDNA library coding for proteins as COOH-terminal fusions with the transcription activation domain of GAL4. Screening of approximately  $1 \times 10^6$  transformants yielded several positive clones. One of the positive clones was found to contain a cDNA insert covering a polypeptide region (amino acid residue 276 to the COOH-terminus, residue 862) of mouse Rabaptin-5. As shown in Fig. I-2B, retransformation of the positive clone [named pGAD-Rbt5 (276-862)] revealed that Rbt5(276-862) was able to interact with  $\gamma$ 1-adaptin (pGBT- $\gamma$ 1) but not with the empty pGBT9 vector. Expectedly,  $\gamma$ 1-adaptin was also able to interact with full-length Rabaptin-5 [Rbt5 (full)]. I also constructed a pGBT9-based vector for Rbt5 (full) and a pGAD-based vector for  $\gamma$ 1-adaptin, cotransformed them into reporter cells, and found that the interaction was positive (data not shown). These results indicate that  $\gamma$ 1-adaptin and Rabaptin-5 are able to interact specifically with each other.

Rabaptin-5 has four potential coiled-coil regions (50, 53); two in the NH<sub>2</sub>-terminal region (CC1-1 and CC1-2) and the other two in the COOH-terminal region (CC2-1 and CC2-2). Rbt5 (276-862) lacks the NH<sub>2</sub>-terminal coiled-coil regions (see Fig. I-2A). In order to determine the region responsible for the interaction with  $\gamma$ 1-adaptin, I therefore divided Rbt5 (276-862) into two regions; one (Rbt5 (276-546)) is the central featureless region and the other (Rbt5 (546-862)) covers the COOH-terminal coiled-coil regions (Fig. I-2A). As shown in Fig. I-2B, Rbt5 (546-862) but not Rbt5(276-546) interacted with  $\gamma$ 1-adaptin. I then constructed Rbt5 (546-728) and Rbt5(662-862) (Fig. I-2A) and found that the former but not the latter interacted with  $\gamma$ 1-adaptin, indicating that at least

the CC2-1 region of Rabaptin-5 is responsible for its interaction with  $\gamma$ 1-adaptin.

I then set out to determine which region of  $\gamma$ 1-adaptin was responsible for its interaction with Rabaptin-5. The  $\gamma$ 1-adaptin polypeptide is structurally divided into two domains; the NH<sub>2</sub>-terminal head or trunk domain and the COOH-terminal ear or appendage domain, which are connected by a proline-rich hinge region (3-5). I therefore constructed pGBT9-based vectors for the head and ear domains and cotransformed either of them with pGAD-Rbt5 (full) into reporter yeast cells. As shown in Fig. I-2C, the ear domain of  $\gamma$ 1-adaptin showed strong interaction with Rabaptin-5. In contrast, the interaction between the head domain and Rabaptin-5 was below the detection level. Because the ear domains of  $\gamma$ 1- and  $\gamma$ 2-adaptins are highly conserved (15), I then examined whether the ear domain of  $\gamma$ 2-adaptin was also able to interact with Rabaptin-5. Expectedly, the ear domain of  $\gamma$ 2-adaptin also showed significant interaction with Rabaptin-5 in the two-hybrid assay (Fig. I-2C). In contrast, the ear domain of  $\alpha$ A-adaptin, which does not show significant homology to that of either  $\gamma$ 1- or  $\gamma$ 2-adaptin, did not show significant interaction.

*In Vitro and in Vivo Interactions between  $\gamma$ 1-Adaptin and Rabaptin-5* — In order to examine whether the interaction between  $\gamma$ 1-adaptin and Rabaptin-5 can be detected biochemically, I prepared fusion proteins between GST and the ear domains of  $\gamma$ 1-,  $\gamma$ 2- and  $\alpha$ A-adaptins, and immobilized them on glutathione-Sepharose beads (In this experiment, a GST fusion protein with  $\alpha$ A-adaptin covering a portion of the hinge region and the ear domain was used in place of the ear domain alone for the reason described in “Materials and Methods.”). Subsequently, the beads were incubated with cytosol and membrane extracts from HeLa cells. In the incubation mixture, GDP or GTP $\gamma$ S was included, because I suspected that a Rab GTPase might regulate the interaction. After washing the beads, I analyzed the bound materials by SDS-PAGE and Western blotting with anti-Rabaptin-5 antibody. As shown in Fig. I-3, a significant

fraction of cytosolic and membrane-associated Rabaptin-5 bound to the GST fusion proteins with the ear domains of  $\gamma$ 1- and  $\gamma$ 2-adaptins (lanes 2, 5, 9 and 12, and lanes 3, 6, 10 and 13, respectively). In contrast, Rabaptin-5 did not bind to the GST fusion protein with the ear domain of  $\alpha$ A-adaptin (lanes 1, 4, 8 and 11) or to GST alone (data not shown), suggesting that the Rabaptin-5 binding is specific to the ear domains of  $\gamma$ 1- and  $\gamma$ 2-adaptins. It is noted that no significant difference was observed in the amount of Rabaptin-5 bound to the GST- $\gamma$ -adaptin-ear fusion between the GDP- and GTP $\gamma$ S-containing conditions. Furthermore, Rab4 or Rab5 was not pulled down with the ear domain.

In an attempt to investigate whether Rabaptin-5 is able to interact with  $\gamma$ 1-adaptin *in vivo*, I subjected postnuclear supernatant from HeLa cells to immunoprecipitation with anti-Rabaptin-5 or anti- $\gamma$ 1-adaptin antibody, and subsequently analyzed by SDS-PAGE and Western blotting with the reversal antibody to examine whether these proteins were coimmunoprecipitated. However, only a faint band for  $\gamma$ 1-adaptin and no band for Rabaptin-5 were detected (data not shown) probably because the antibodies used did not work well to immunoprecipitate the endogenous proteins. I therefore established a HeLa cell line stably expressing HA-tagged Rabaptin-5 (HeLa/HA-Rbt5), prepared postnuclear supernatant from this cell line, and subjected it to immunoprecipitation with anti-HA or anti-Rabaptin-5 antibody. As shown in Fig. I-4, subsequent SDS-PAGE and Western blotting with anti- $\gamma$ 1-adaptin antibody revealed that  $\gamma$ 1-adaptin was coimmunoprecipitated with both the anti-HA and anti-Rabaptin-5 antibodies (lanes 3 and 5, respectively). When postnuclear supernatant from non-transfected HeLa cells were subjected to immunoprecipitation with anti-HA and anti-Rabaptin-5 antibodies, no band (lane 2) and a faint band (lane 4) for  $\gamma$ 1-adaptin, respectively, were detected. Essentially the same results were obtained using postnuclear supernatant from HeLa/HA-Rbt5 cells transiently overexpressing Rab4(Q67L) or Rab5(Q79L) (data not shown). These results indicate that the interaction between  $\gamma$ 1-adaptin

and Rabaptin-5 specifically occurs *in vivo*.

*Rabaptin-5 Colocalizes with  $\gamma$ 1-Adaptin in the Perinuclear Region* — It has been shown, by application of an improved fixation method of cells (63), that endogenous Rabaptin-5 is localized to not only punctate but also perinuclear endosome-like structures (64). On the other hand,  $\gamma$ 1-adaptin has been shown to localize to endosome-like structures as well as the TGN (7-10). I therefore examined whether  $\gamma$ 1-adaptin and Rabaptin-5 colocalize in the cell by double staining for the endogenous proteins. In HeLa cells (Fig. I-5, A-A") and NRK cells (B-B"), both of which were fixed and permeabilized by the method of Neuhaus *et al.* (63; see "Materials and Methods"), the staining for Rabaptin-5 was found to be in the perinuclear region, where the staining was overlapped with that for  $\gamma$ 1-adaptin, although cytoplasmic staining for Rabaptin-5 was also apparent.

I then treated the cells with BFA, a fungal metabolite, and observed the distribution of  $\gamma$ 1-adaptin and Rabaptin-5. BFA is known to inhibit guanine nucleotide exchange factors for ADP-ribosylation factor (ARF) and thereby inhibit membrane binding of ARF (for review, see Refs. 65, 66). Because association of the AP-1 complex onto membranes is dependent on ARF, treatment of cells with BFA causes dissociation of AP-1 from membranes (67-69). Although BFA also causes redistribution of transmembrane Golgi proteins, the redistribution requires much longer BFA treatment (more than 5 min) than that required for dissociation of coat proteins from membranes (within 30 sec) (69). It was therefore speculated that a relatively short-term treatment of cells with BFA gave rise to redistribution of not only  $\gamma$ 1-adaptin but also Rabaptin-5 into the cytoplasm if membrane association of Rabaptin-5 was mediated by its binding to  $\gamma$ 1-adaptin. As shown in Fig. I-5, C-C", this was the case; when NRK cells were treated with 5  $\mu$ g/ml BFA for 1 min, both  $\gamma$ 1-adaptin and Rabaptin-5 were redistributed from the perinuclear region to the cytoplasm. In contrast, such a treatment did not affect the distribution of a Golgi-resident protein,

mannosidase II, nor that of a peripheral early endosomal protein, EEA1 (data not shown), indicating that the effect of the short-term BFA treatment is specific for  $\gamma$ 1-adaptin and Rabaptin-5. Thus, membrane association of  $\gamma$ 1-adaptin and Rabaptin-5 appeared to be a coupled event. Taken together with the above data on the interaction between  $\gamma$ 1-adaptin and Rabaptin-5, it seems likely that membrane association of Rabaptin-5 is dependent on  $\gamma$ 1-adaptin, although a formal possibility that the Rabaptin-5 association is directly regulated by ARF cannot be rigorously excluded.

*Localization of  $\gamma$ 1-Adaptin on Endosomal Compartments* — I then set out to examine whether  $\gamma$ 1-adaptin is localized on endosomes in my system. To this end, I took two approaches. First, I compared the distribution of  $\gamma$ 1-adaptin with that of internalized transferrin, because it is known to reach early endosomes at earlier time points of internalization and recycling compartments at later points, then return to the cell surface (for review, see Ref. 70). As shown in Fig. I-6, after 2 min of internalization, Alexa594-conjugated transferrin was found in punctate endosomal structures distributed throughout the cytoplasm. At this time point, there was little overlap between transferrin and  $\gamma$ 1-adaptin (A-A"). After 10 min of internalization, however, Alexa594-transferrin began to accumulate not only in peripheral punctate structures but also in perinuclear structures (data not shown). After 20 min of internalization, the transferrin labeling was significantly superimposed on the perinuclear  $\gamma$ 1-adaptin-containing structures (B-B"). Second, I exploited the fact that overexpression of Rab5(Q79L) or Rab4(Q67L) leads to exaggeration of structures containing Rabaptin-5 and its variant Rabaptin-4 (50, 57), although Rab5 and Rab4 are localized to distinct but partially overlapping endosomal compartments, peripheral early endosomes and perinuclear recycling endosomes, respectively (57, 58, 60). In HeLa cells overexpressing HA-Rab4(Q67L), the small GTPase and  $\gamma$ 1-adaptin colocalized significantly, although partially, on perinuclear structures (C-C"). In contrast, localization of  $\gamma$ 1-adaptin on exaggerated early

endosomal structures containing overexpressed Rab5(Q79L) was barely observable (D-D"). These observations indicate that at least a population of  $\gamma$ 1-adaptin molecules is localized on endocytic compartments, probably recycling endosomes, as well as on the TGN.



## DISCUSSION

The present study provides the first evidence for a direct interaction between  $\gamma$ -adaptins and Rabaptin-5. In a yeast two-hybrid screening, I found that  $\gamma$ 1-adaptin is able to interact with Rabaptin-5. Further two-hybrid analysis (Fig. I-2) and pull down assay (Fig. I-3) showed that the ear domains of both  $\gamma$ 1- and  $\gamma$ 2-adaptins interact with the CC2-1 region of Rabaptin-5. The physiological significance of the interaction between  $\gamma$ 1-adaptin and Rabaptin-5 is corroborated by the results that Rabaptin-5 and  $\gamma$ 1-adaptin can be coimmunoprecipitated from cell lysates (Fig. I-4) and that immunofluorescence analysis revealed their significant colocalization on perinuclear structures, probably on recycling compartments (Figs. I-5 and I-6). However, I was unable to examine the physiological relevance of the interaction between  $\gamma$ 2-adaptin and Rabaptin-5 due to the limitation of antibodies to  $\gamma$ 2-adaptin raised in our lab, which do not work well in immunoprecipitation nor detect the endogenous protein in immunofluorescence analysis (15).

On the basis of the data presented here, at least two explanations are possible for the role of Rabaptin-5 in the function of clathrin-coated vesicles containing the AP-1 complex. One is that clathrin-coated vesicles that are derived from the TGN become associated with Rabaptin-5 either in the cytosol or on membranes, which in turn leads to docking and fusion of the vesicles with endosomes by forming oligomeric complexes with EEA1, Rabex-5, and NSF (54). This possibility is indirectly supported by the recent report of Rubino *et al.* showing that docking and fusion between plasma membrane-derived clathrin-coated vesicles and early endosomes requires prior recruitment of Rabaptin-5 onto both membranes and that of EEA1 onto endosomal membranes (71). It is therefore tempting to speculate that TGN-derived clathrin-coated vesicles associated with Rabaptin-5 are also competent to dock and fuse with endosomes. Recent data showing that EEA1 directly

interacts not only with syntaxin-13 (54), a SNARE implicated in plasma membrane-early endosome trafficking (54, 71, 72), but also with syntaxin-6 (55), a SNARE that is associated with TGN-derived clathrin-coated vesicles and is implicated in TGN-endosome trafficking (73), is in line with this speculation.

The other possible explanation is that Rabaptin-5 is associated with endosome-derived clathrin-coated vesicles. Although AP-1 is associated mainly with the TGN, it has been shown to be also associated with endosomes (7-10). The present study shows that at least a population of AP-1 localizes on Rab4-containing recycling compartments (Fig. I-6). Furthermore, most recent study using cells derived from mice lacking the  $\mu$ 1 subunit of the AP-1 complex has unexpectedly highlighted the crucial role of AP-1 in retrograde endosome to TGN trafficking, rather than in anterograde TGN to endosome trafficking, of MPRs (32). Taken together, it is possible that clathrin-coated vesicles derived from endosomes may dock and fuse with the TGN or other compartment(s) through their association with Rabaptin-5.

In either case, it is an interesting issue whether the interaction between  $\gamma$ 1-adaptin and Rabaptin-5 is regulated by Rab GTPases, because Rabaptin-5 and its variant Rabaptin-4 interact with GTP-bound Rab5 and Rab4 (50, 56, 57) and because recruitment of Rabaptin-5 onto early endosomes and plasma membrane-derived clathrin-coated vesicles is dependent on Rab5 (71). Furthermore, McLauchan *et al.* have shown that a complex of Rab5 and guanine-nucleotide dissociation inhibitor is required for plasma membrane clathrin-coated pits to sequester ligand in an adaptor-dependent manner and suggested that recruitment of components essential for vesicle targeting and fusion is coupled to the formation of functional transport vesicles (74). My immunofluorescence analysis indicates that at least a population of  $\gamma$ 1-adaptin molecules is localized to recycling compartments containing Rab4(Q67L), but not to early endosomes containing Rab5(Q79L) (Fig. I-6). This observation is

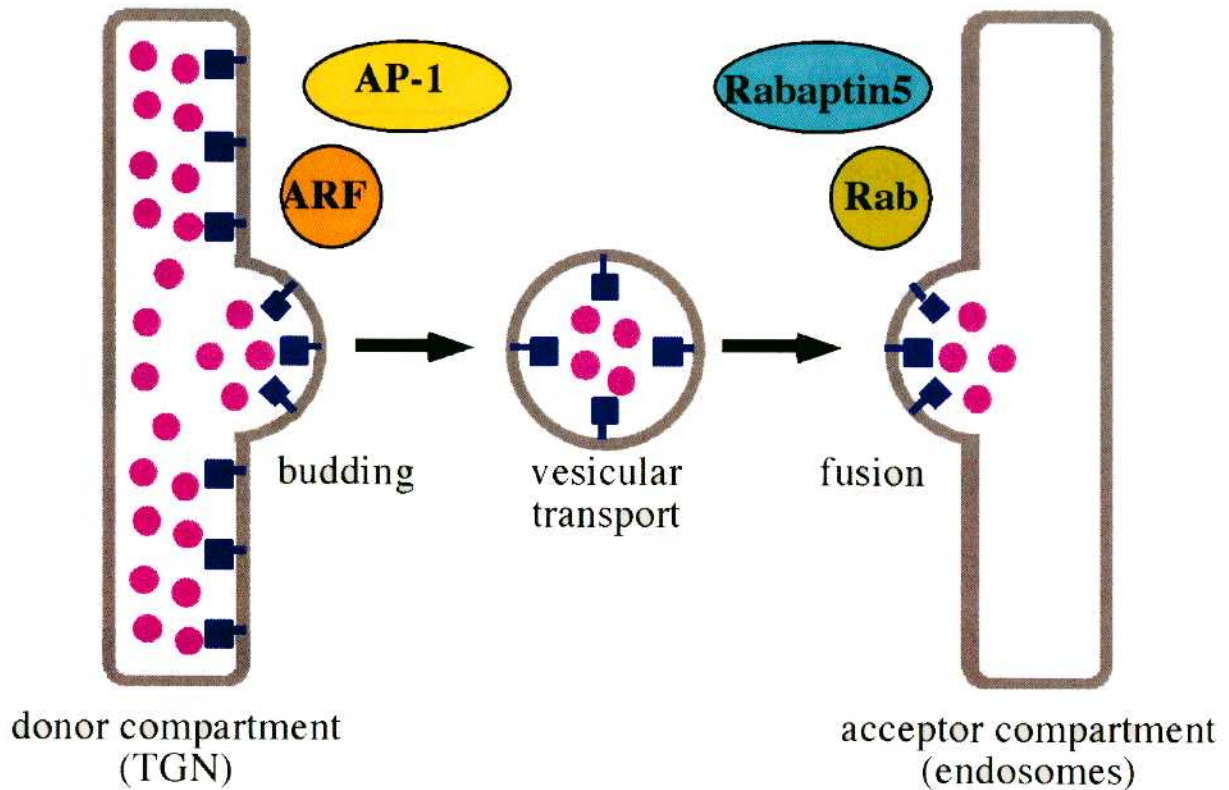
in line with evidence for association of AP-1 with GLUT4-containing vesicles (75), with which Rab4 is also known to associate (76). It is therefore possible that Rab4 may regulate recruitment of Rabaptin-5/Rabaptin-4 onto nascent clathrin/AP-1-coated vesicles. However, my biochemical analyses failed to show the direct involvement of the Rab GTPase in the regulation of the  $\gamma$ 1-adaptin-Rabaptin-5 interaction. First, the GST fusion protein with the  $\gamma$ 1-adaptin-ear domain pulled down Rabaptin-5 to the same extent under GDP- and GTP $\gamma$ S-containing conditions (Fig. I-3). Second, the GST- $\gamma$ 1-adaptin-ear fusion protein did not pull down Rab4 or Rab5 together with Rabaptin-5 (data not shown). Finally, my preliminary experiment revealed that overexpression of Rab4(Q67L) or Rab5(Q79L) did not affect the coimmunoprecipitation efficiency of Rabaptin-5 and  $\gamma$ 1-adaptin.

Christoforidis *et al.* have proposed, on the basis of their data showing that EEA1 alone can support docking and fusion between endosomes and the Rabaptin-5/Rabex-5 complex enhances the fusion efficiency, that the Rabaptin-5/Rabex-5 complex may ensure the activation of Rab5 on endosomes and the activated Rab5 may in turn regulate EEA1 recruitment and activity (52). Furthermore, Cao and Barlowe have recently shown, by an *in vitro* docking and fusion assay using combinations of vesicles and target membranes derived from wild-type yeast cells and temperature-sensitive mutants, that Ypt1p, a yeast ortholog of Rab1, is required on target membranes and not on vesicles for the membrane docking and fusion (77, reviewed in Ref. 78). Taken together, it is possible that the Rabaptin-5/Rabex-5 complex associated with clathrin-coated vesicles may regulate Rab4 on target membranes rather than Rab4 regulates the Rabaptin-5 association onto vesicles. However, I was unable to show evidence for association with  $\gamma$ 1-adaptin of Rabex-5 together with Rabaptin-5 due to unavailability of anti-Rabex-5 antibody and it is currently unknown whether Rabex-5 is also active on Rab4 due to a high, intrinsic guanine-nucleotide exchange rate of Rab4 *in vitro* (79). Further

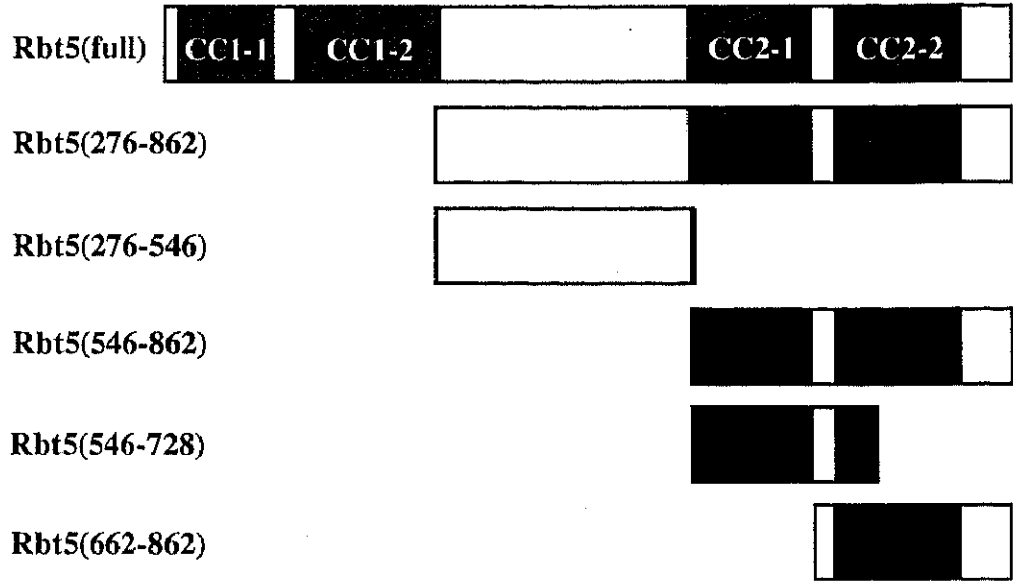
experiments will be required to address this issue.

Most recently, a family of proteins, designated as GGA1, GGA2/Vear and GGA3, that have commonly a COOH-terminal domain homologous to the ear domain of  $\gamma$ -adaptin have been identified and shown to localize on the *trans*-Golgi and/or TGN (33-37). Furthermore, the ear-like domains of the GGA proteins have been shown to interact with  $\gamma$ -synergin (35, 37), that is known to interact with the ear domain of  $\gamma$ -adaptin (26). It is therefore an interesting issue whether the GGA ear-like domains are also able to interact with Rabaptin-5. A preliminary two-hybrid analysis of our group indicates that such an interaction can occur, suggesting that the ear (ear-like) domains of  $\gamma$ -adaptins and GGAs, like that of  $\alpha$ -adaptin, may regulate membrane trafficking by interacting with various regulatory molecules.

## FIGURES

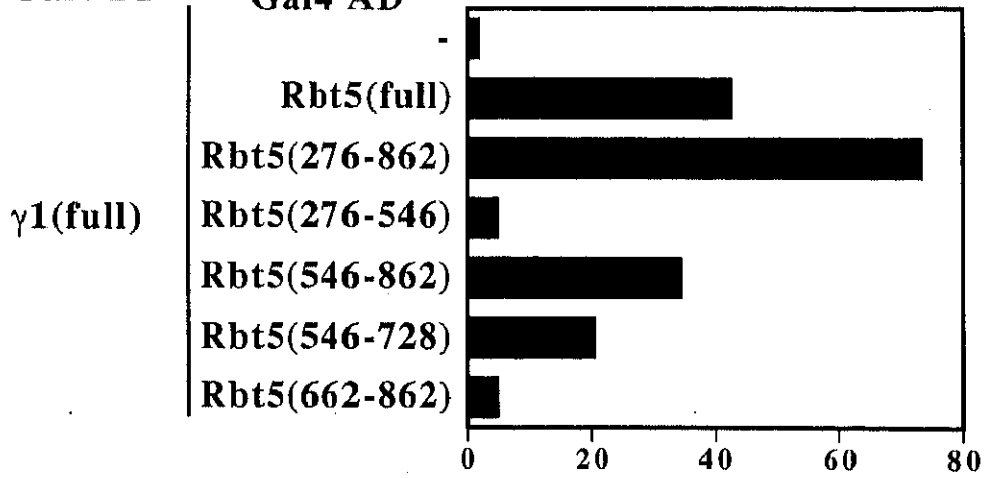


**Fig. I-1. Transport between organelle.** Vesicular carriers that capture cargo molecules buds off from one compartment (donor compartment) and deliver the contents by fusing with another compartment (acceptor compartment). Transport vesicle formation starts by small GTPase ARF, and the fusion events are regulated by another small GTPase Rab. Upon cycles of GDP- and GTP-bound states, these GTPases undergo a conformational changes. When bound to GDP, GTPases have a low affinity for membranes, but when this is exchanged for GTP, the membrane-binding conformation of the protein is stabilized. The GTP-bound form binds and activates specific effector molecules, which induce a cellular response (membrane budding and fusion).

**A****B**

Gal4 BD

Gal4 AD

**C** $\gamma$ 1(full) $\gamma$ 1(head) $\gamma$ 1(ear) $\gamma$ 2(ear) $\alpha$ A(ear)

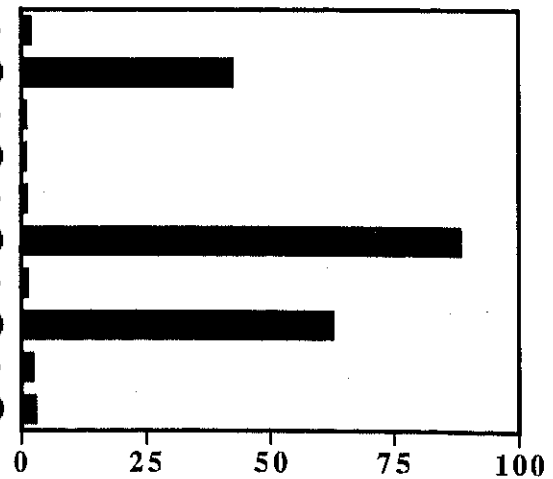
Rbt5(full)

Rbt5(full)

Rbt5(full)

Rbt5(full)

Rbt5(full)

relative  $\beta$ -galactosidase units

**Fig. I-2. Interaction between  $\gamma$ -adaptin and Rabaptin-5 revealed by the yeast two-hybrid system.** *A*, Schematic representation of structures of mouse Rabaptin-5 (Rbt5) and its deletion mutants used. *B*, Interaction between full-length  $\gamma$ 1-adaptin and Rabaptin-5 or its deletion mutants. Reporter yeast cells cotransformed with the pGBT9-based (GAL4 BD) full-length  $\gamma$ 1-adaptin vector and either of the pGAD10-based (GAL4 AD) Rabaptin-5 vectors as indicated were subjected to liquid  $\beta$ -galactosidase assay as described under “materials and methods”. *C*, Interaction between adaptin fragments and full-length Rabaptin-5. Reporter yeast cells cotransformed with either of the pGBT9-based adaptin vectors as indicated and the pGAD10-based full-length Rabaptin-5 vector or empty vector were assayed as described above.

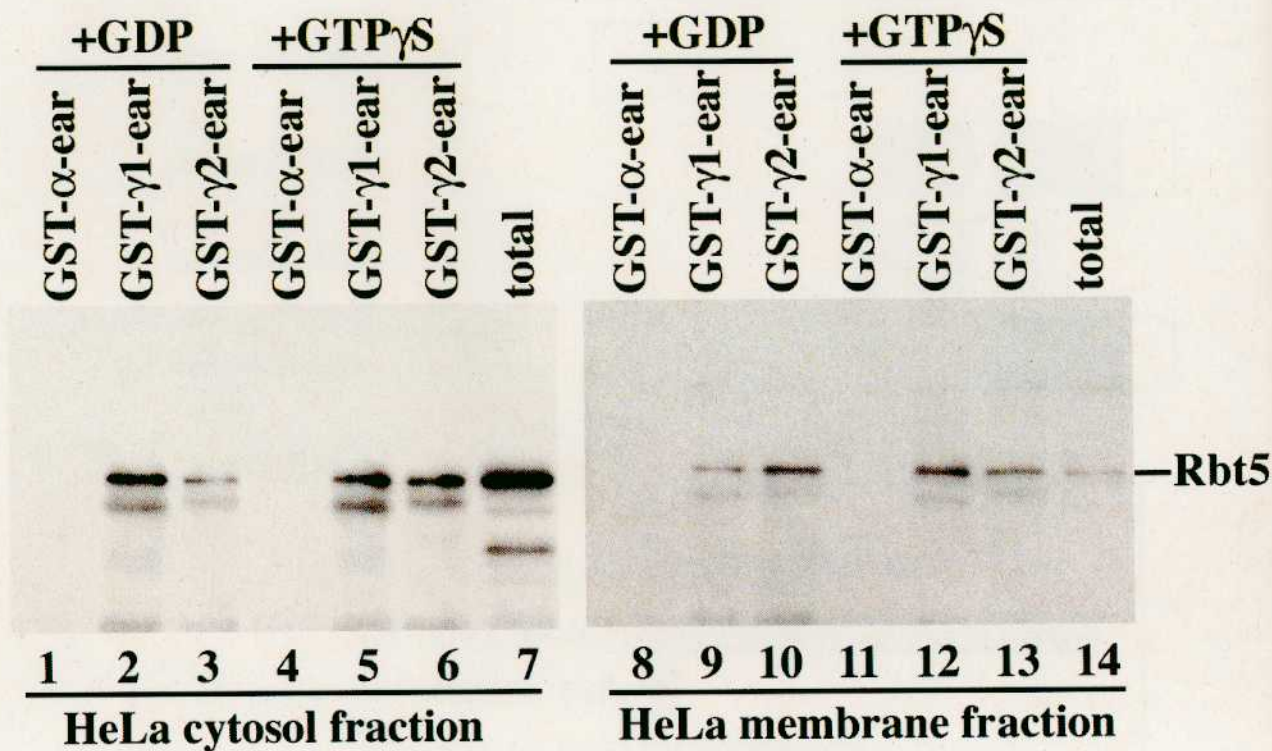


**Fig. I-3. Pull down assay.** The ear domain of  $\gamma 1$ -,  $\gamma 2$ - or  $\alpha A$ -adaplin fused to GST as indicated was immobilized on glutathione-Sepharose beads, incubated with cytosol or membrane extract from HeLa cells in the presence of GDP or GTP  $\gamma S$ , and subjected to Western blotting with anti-Rabaptin-5 antibody as described under "Materials and Methods" to study their *in vitro* binding to Rabaptin-5.



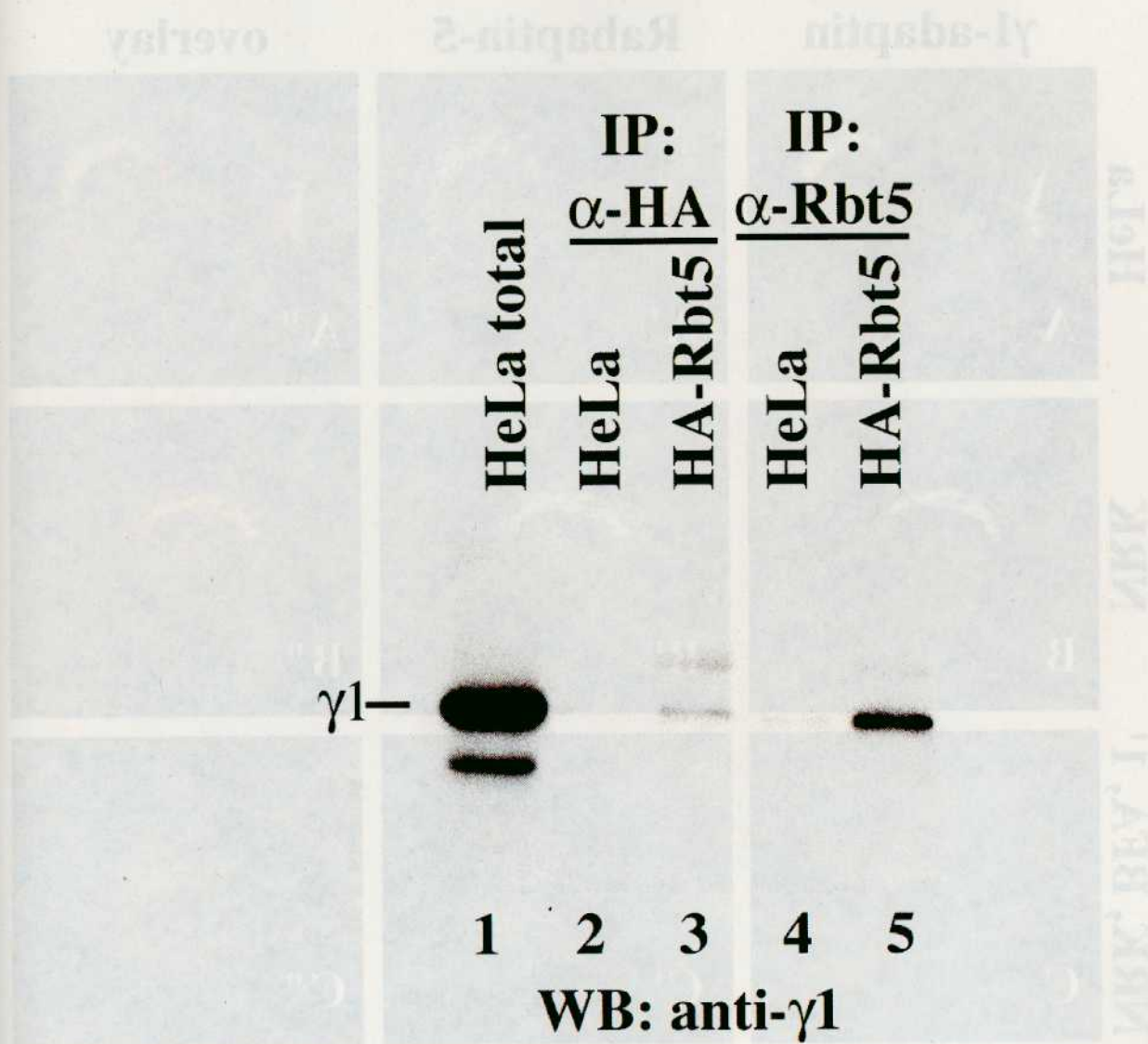


**Fig. I-4. Coimmunoprecipitation analysis.** Lysates from HeLa cells or HeLa/HA-Rbt5 cells were immunoprecipitated (IP) with anti-HA ( $\alpha$ -HA) or anti-Rabaptin-5 ( $\alpha$ -Rbt5) antibody and the immunoprecipitates were subjected to Western blotting (WB) with anti- $\gamma$ 1-adaptin as described under "Materials and Methods" to study the in vivo interaction between  $\gamma$ 1-adaptin and Rabaptin-5.

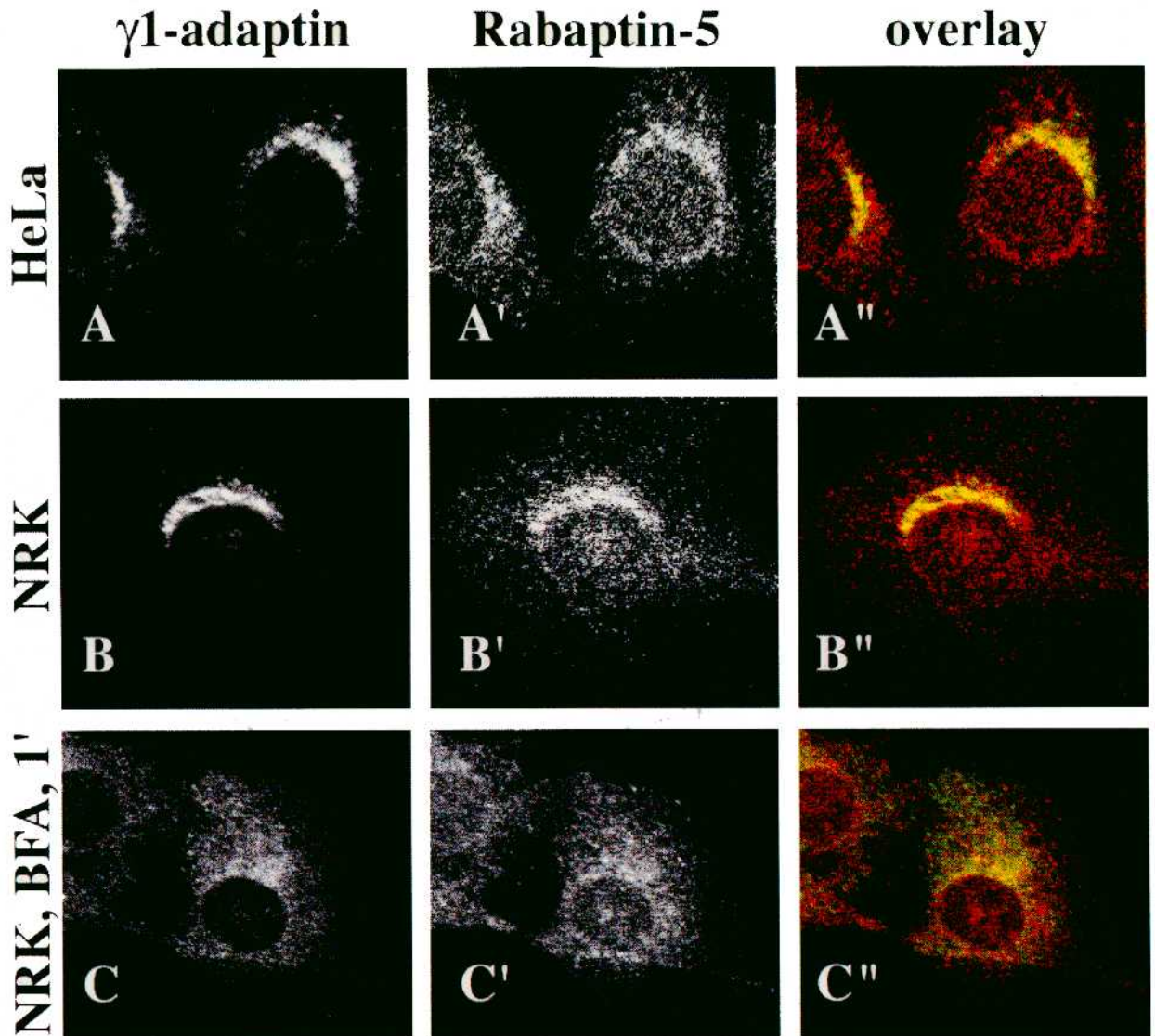


**Fig. I-5. Colocalization of endogenous  $\gamma$ 1-adaptin and Rabaptin-5.** HeLa cells (A-A'') or NRK cells (B-B'' and C-C'') were directly fixed (A-A'' and B-B'') or incubated with 5 $\mu$ g/ml BFA for 1 min prior to fixation (C-C'') and were subjected to double-staining for  $\gamma$ 1-adaptin (A, B and C) and Rabaptin-5 (A', B' and C') as described under "materials and methods". Overlays are shown in A'', B'' and C'' (green for  $\gamma$ 1-adaptin and red for Rabaptin-5).

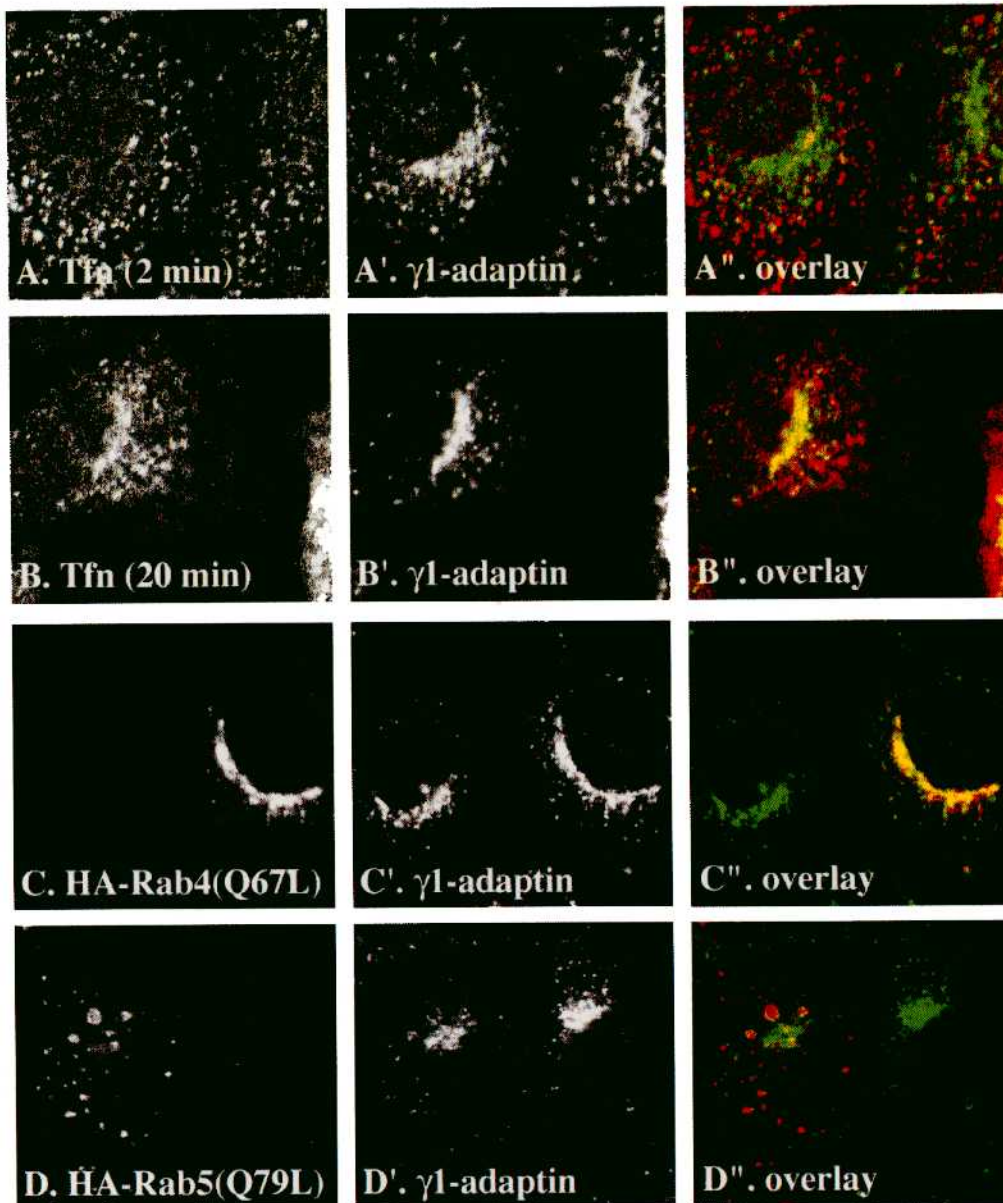


**Fig. I-6. Localization of  $\gamma$ 1-adaptin on endosomes.** *A* and *B*, HeLa cells preloaded with Alexa594-conjugated transferrin (Tfn; *A* and *B*) were incubated at 37 °C for 2 (*A-A''*) or 20 (*B-B''*) min, fixed and processed for immunofluorescence to visualize  $\gamma$ 1-adaptin (*A'* and *B'*) as described under “materials and methods”. *C* and *D*, HeLa cells transfected with pcDNA3-HA-Rab4 (Q67L) (*C-C''*) or pcDNA3-HA-Rab5 (Q79L) (*D-D''*) were subjected to double-staining with anti-HA (*C* and *D*) and anti- $\gamma$ 1-adaptin (*C'* and *D'*) antibodies as described under “materials and methods”. Overlays are shown in *A''-D''* (green for  $\gamma$ 1-adaptin and red for transferrin or HA-Rab).